

# Increased gene dosage and mRNA expression from chromosomal duplications in *Caenorhabditis elegans*

Bhavana Ragjipani , Sarah Elizabeth Albritton , Ana Karina Morao , Diogo Mesquita, Maxwell Kramer , Sevinç Ercan \*

Department of Biology, Center for Genomics and Systems Biology, New York University, New York, NY 10003, USA

\*Corresponding author: Department of Biology, Center for Genomics and Systems Biology, New York University, New York, NY 10003, USA. Email: se71@nyu.edu

## Abstract

Isolation of copy number variations and chromosomal duplications at high frequency in the laboratory suggested that *Caenorhabditis elegans* tolerates increased gene dosage. Here, we addressed if a general dosage compensation mechanism acts at the level of mRNA expression in *C. elegans*. We characterized gene dosage and mRNA expression in 3 chromosomal duplications and a fosmid integration strain using DNA-seq and mRNA-seq. Our results show that on average, increased gene dosage leads to increased mRNA expression, pointing to a lack of genome-wide dosage compensation. Different genes within the same chromosomal duplication show variable levels of mRNA increase, suggesting feedback regulation of individual genes. Somatic dosage compensation and germline repression reduce the level of mRNA increase from X chromosomal duplications. Together, our results show a lack of genome-wide dosage compensation mechanism acting at the mRNA level in *C. elegans* and highlight the role of epigenetic and individual gene regulation contributing to the varied consequences of increased gene dosage.

**Keywords:** gene dosage; copy number; dosage compensation; X chromosome; RNA-seq; DNA-seq; chromosome duplications; *Caenorhabditis elegans*; modENCODE; gene expression

## Introduction

Chromosomal aneuploidies or copy number variations (CNVs) are associated with a wide range of phenotypes in many organisms (Tang and Amon 2013; Durrbaum and Storchova 2016). To understand the effect of gene dosage on gene expression, a series of studies compared DNA copy number and mRNA levels in aneuploid cells and animals (Kojima and Cimini 2019). In plants and mammalian cells, partial and full aneuploidies showed complex responses to alterations in gene dosage, with secondary effects on the transcriptome and nonlinear correlation between copy number and expression (Ait Yahya-Graison et al. 2007; Huettel et al. 2008). In *Drosophila melanogaster*, buffering mechanisms were proposed to act through the gene regulatory networks to dampen the effect of gene dosage (Zhang et al. 2010; Malone et al. 2012). In *Saccharomyces cerevisiae*, gene expression largely correlated with copy number with some variation between genes (Gasch et al. 2016; Torres et al. 2016; Taggart and Li 2018).

While there is no effective compensation of chromosomal aneuploidies for the rest of the genome, X chromosomes are highly regulated in many animals. Typically, females (XX) contain twice the number of X chromosomes than males (XY) but the 2 sexes express similar levels of X chromosomal transcripts. Strategies that equalize X chromosome expression between sexes differ in different animals. In mammals (human and mouse), one of the X chromosomes is silenced in XX females; in

flies (*Drosophila*), the single X chromosome is upregulated by a factor of 2 in XY males; and in worms (*Caenorhabditis*), both X chromosomes are downregulated by a factor of 2 in XX hermaphrodites (Meyer 2005; Samata and Akhtar 2018; Dossin and Heard 2021). While strategies differ, in each system, a multisubunit protein complex specifically targets and regulates X chromosome transcription in one of the 2 sexes through epigenetic mechanisms (Ercan 2015).

A high rate of CNVs was reported in mutation accumulation experiments in *Caenorhabditis elegans* (Lipinski et al. 2011; Konrad et al. 2018). In addition, 80% of the genome could be isolated as chromosomal duplications in the laboratory, leading to the conclusion that the worm is relatively tolerant to increased gene dosage (Hodgkin 2005). To understand the effect of increased gene dosage in *C. elegans*, we characterized large chromosomal duplications in several strains using DNA-seq and analyzed the effect of increased gene dosage in 3 chromosomal duplications and 1 fosmid insertion strain using mRNA-seq. Like other species, there was a complex response to increased gene dosage in *C. elegans*. While the average mRNA level increased for genes located within large duplications and the integrated fosmid, genes within the same chromosomal duplication showed varying levels of mRNA increase. An X chromosomal duplication that recruits the somatic dosage compensation complex (DCC) showed lower mRNA increase compared to one that did not recruit, also demonstrating the contribution of epigenetic regulation to the effect of gene dosage.

Received: May 13, 2022. Accepted: June 09, 2022

© The Author(s) 2022. Published by Oxford University Press on behalf of Genetics Society of America.

This is an Open Access article distributed under the terms of the Creative Commons Attribution License (<https://creativecommons.org/licenses/by/4.0/>), which permits unrestricted reuse, distribution, and reproduction in any medium, provided the original work is properly cited.

## Materials and methods

### Strains

Unless otherwise noted, strains were maintained at 20°C on nematode growth medium agar plates using standard *C. elegans* growth methods. TY1916 [yDp11 (X; IV); lon-2(e678) unc-9(e101) X] contains duplication (yDp11), producing long, non-Unc homozygous hermaphrodites. SP117 [mnDp10 (X; I); unc-3(e151) X] produces wild-type looking homozygous hermaphrodites. SP219 [mnDp1 (X; V)/+ V; unc-3(e151) X] contains the duplication (mnDp1), which is homozygous lethal, thus, wild-type looking heterozygous hermaphrodites containing the duplication were picked. BC4289 [sDp10 (IV; X)] contains the homozygous-viable duplication (sDp10). SP1981 [unc-115(mn481) dpy-6(e14) X; stDp2 (X; II)/+] contains homozygous-lethal duplication (stDp2). Wild-type looking heterozygous hermaphrodites were picked. VC100 [unc-112(r367) V; gkDf2 X] contains the homozygous-viable deletion (gkDf2) and produces wild-type looking hermaphrodites. OP37 {wgsIs37 [pha-4::TY1::EGFP::3xFLAG + unc-119(+)]} is wild-type looking and generated by Sarov et al. (2012).

### DNA-seq

At least 20 worms were hand-picked as young adults. Worms were washed by settling animals at least 3 times with 1 ml M9 and starved overnight to remove gut bacteria. Following a final M9 wash, worms were resuspended in 100 µl TE and frozen. For DNA isolation, 400 µl of lysis buffer (0.1 M Tris-HCl; 0.1 M NaCl; 50 mM EDTA; 1.25% SDS) was added and worms were sonicated using Bioruptor 30 s on/off at high for 30 min. Sonicated DNA was isolated using Qiagen MinElute kit and Illumina DNA sequencing libraries were prepared as described previously (Albritton et al. 2014). Single- or paired-end sequencing was performed using Illumina HiSeq-2000 and aligned to genome version WS220 (ce10) using Bowtie2 (version 2.3.2) with default settings (Langmead and Salzberg 2012). All replicate and read number information is provided in Supplementary File 1. Samtools version 1.6 (Li 2011) was used to merge replicates before running bamCompare from Deeptools version 3.3.1 (Ramírez et al. 2016), using the following options: `-binSize 500, -scaleFactorsMethod None, -normalizeUsing CPM, -operation log2, -minMappingQuality 30, -outFileFormat bedgraph, and -ignoreDuplications`. Copy number analysis was performed with CNVnator version 0.3.3 (Abyzov et al. 2011) comparing data from mutant strains to reference genome WS220 (ce10) using `bin_size=1,000`. CNVnator output files listing deletions and duplications are provided in Supplementary File 2. Overlap of CNVs with genes was determined by Galaxy (<https://usegalaxy.org/>) tools using coverage option in “Operate on Genomic Intervals” (Afgan et al. 2018) and provided in Supplementary File 3. Only genes within the duplications and deletions greater than 10 kb were considered for further analysis.

### mRNA-seq

Mixed-stage embryos were collected from N2, TY1916, BC4289 and SP117 by bleaching gravid adults. L2-L3 worms were collected by plating embryos and growing for 22–26 h at 22.5°C, and young adults next day. Worms were resuspended in at least 10 volumes of Trizol and stored at –80°C. RNA preparation was performed as previously (Albritton et al. 2014). Briefly, samples were freeze cracked 3–5 times, followed by TRIzol purification, and cleaned up with Qiagen RNeasy kit. From 0.5 to 10 µg of total RNA, mRNA was purified using Sera-Mag oligo(dT) beads (Thermo Scientific), sheared and stranded Illumina sequencing

libraries were prepared using a previously published protocol (Parkhomchuk et al. 2009). Sequencing was performed with Illumina HiSeq-2000 and reads were aligned to genome version WS220 with Hisat2 version 2.2.1 (Kim et al. 2019) using default parameters. Count data were calculated using HTSeq version 0.13.5 (Putri et al. 2022) and differential expression was performed using the R package DESeq2 version 1.30.1 (Love et al. 2014). FPKM values were generated using Cufflinks version 2.2.1 with options `-p 8 -library type fr- first strand` (Trapnell et al. 2010). FPKM and DESeq2 output are provided in Supplementary File 4. In Fig. 3, log<sub>2</sub> fold change values were median centered by subtracting the genome median from each value.

### Gene enrichment analysis in OP37

Genes differentially expressed in OP37 compared to N2 were analyzed using the Wormbase tool Gene Set Enrichment Analysis (Angeles-Albores et al. 2016). PHA-4 ChIP-seq binding peaks from OP37 L3 larvae were downloaded from the modERN project (Kudron et al. 2018). The results of the enrichment analyses and the list of differentially expressed genes are provided in Supplementary File 5.

## Results

### Characterization of chromosomal duplications and deletions using DNA-seq

To analyze the effect of gene dosage on mRNA expression, we used previously isolated strains with megabase-scale duplications (Supplementary File 1). Since prior characterization of the duplications was done by visible genetic markers (Hodgkin 2005; Edgley et al. 2006), we performed DNA-seq to map genes that were duplicated or deleted. First, we calculated average read coverage within 1-kb windows tiled across the genome. Plotting the ratio of coverage to wild type confirmed previously mapped duplications (Fig. 1).

To further characterize the strains, we used CNVnator to generate a list of genomic windows with increased and decreased coverage compared to N2 (Abyzov et al. 2011; Supplementary File 2). In addition to the mapped changes, many of the strains showed smaller CNVs that were different from the N2 strain (Fig. 2). Some CNVs were common among the duplication strains, which may have originated from a laboratory strain polymorphic to N2 (Vergara et al. 2009). Notably, there were multiple smaller deletions and insertions within and at the boundaries of the larger duplications (Supplementary File 2). One example is the presence of a duplication near ~40 kb deletion on the X chromosome in the VC100 strain. The presence of additional changes in the boundaries may be due to imperfect repair of the double-strand breaks used to induce aneuploidies, followed by selection to laboratory conditions (Farslow et al. 2015).

### Increased gene dosage and mRNA expression from chromosomal duplications

To analyze the effect of chromosomal duplications on gene expression, we performed mRNA-seq in 2 homozygous-viable strains with various length and number of duplications. SP117 contains a ~5 Mb X chromosomal duplication attached to chromosome I (mnDp10). TY1916 contains a ~1 Mb duplication from the X chromosome attached to chromosome IV (yDp11). TY1916 also contains previously uncharacterized changes involving the right arm of chromosome IV and the left end of chromosome V (Fig. 1). The left tip of chromosome V coverage (0.67) is similar to that of the characterized duplication from the X chromosome

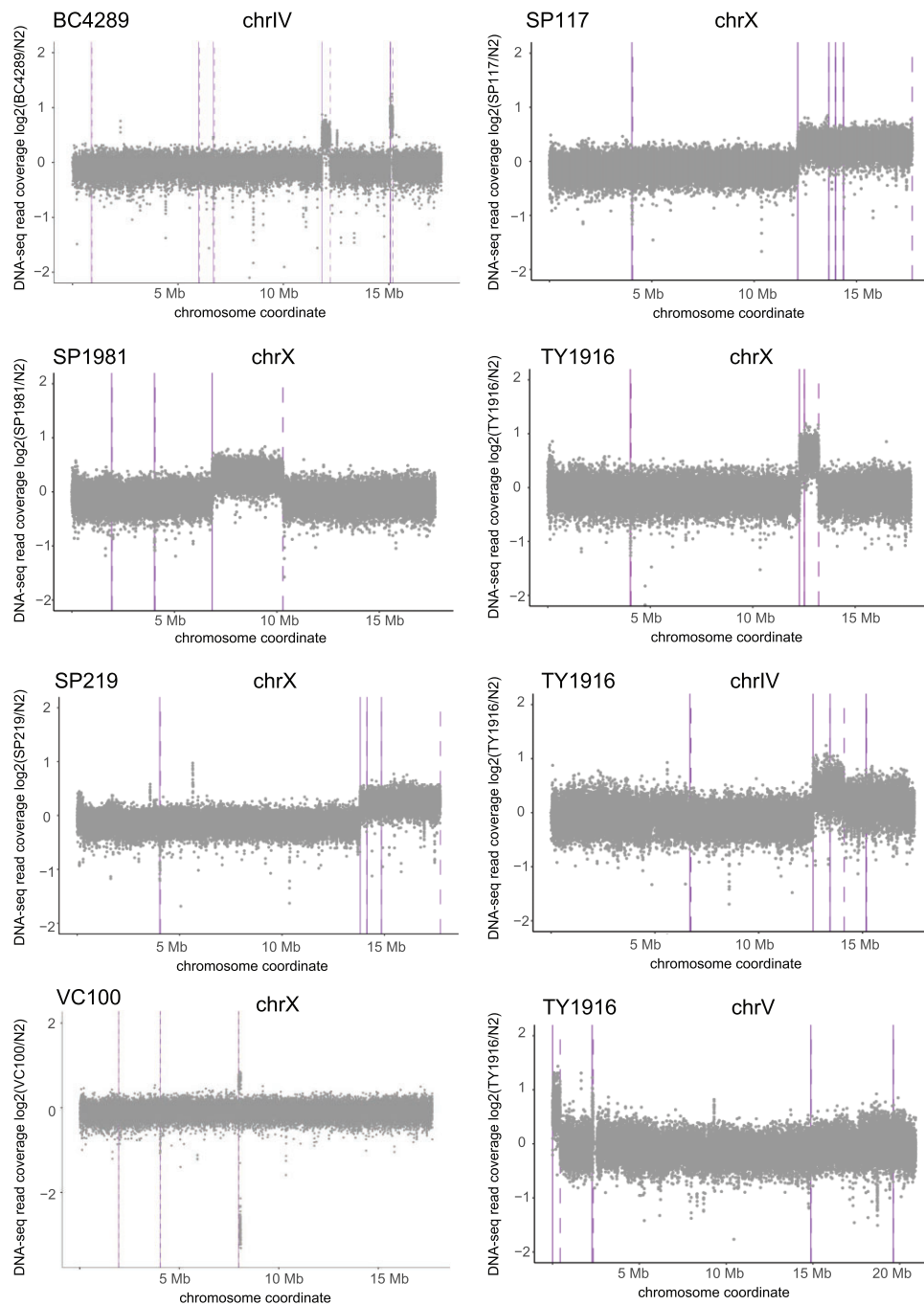


**Fig. 1.** DNA-seq analysis of large chromosomal duplications. The x-axes are coordinates across the chromosomes containing duplications in each strain. The y-axis is  $\log_2(\text{mutant}/N_2)$  coverage [CPM (counts per million) normalized and averaged for 1-kb windows]. Solid vertical lines indicate the start of a duplication and dotted lines indicate the end of a duplication as determined by CNVnator output.

(0.60), thus appears to be duplicated. In the case of region with increased coverage on chromosome IV, the median ratio of coverage is lower (0.40) than that of the X duplication (0.60), thus this region may be present as free duplication or heterozygous in the population of worms used for DNA-seq.

To identify the genes affected by the chromosomal duplications, we used the CNVnator defined regions and categorized genes as duplicated or deleted (if transcription start-end of the gene fully overlaps with the CNV), affected (if overlap is 1 bp or more), or unaffected (no overlap; Supplementary File 3). We then plotted the  $\log_2$  ratio of mRNA coverage in the duplicated strain compared to control along the wild-type chromosomes,

highlighting genes within each category. Across all duplications, average mRNA-seq expression was increased, suggesting that gene dosage correlates with mRNA expression in *C. elegans* (Fig. 3). Notably, the effect on individual genes was variable, showing a range of  $\log_2$  ratios for genes located within the same duplication (Supplementary File 4).

In mRNA-seq analyses using ratios, inclusion of lowly expressed genes reduces the magnitude of observed effect (Deng et al. 2011). To address this problem, we filtered out genes with FPKM values less than 1 in any wild-type replicate, and replotted the 3 large duplications in SP117 and TY1916 (Supplementary Fig. 1a). The median mRNA-seq increase for all 3 duplications was

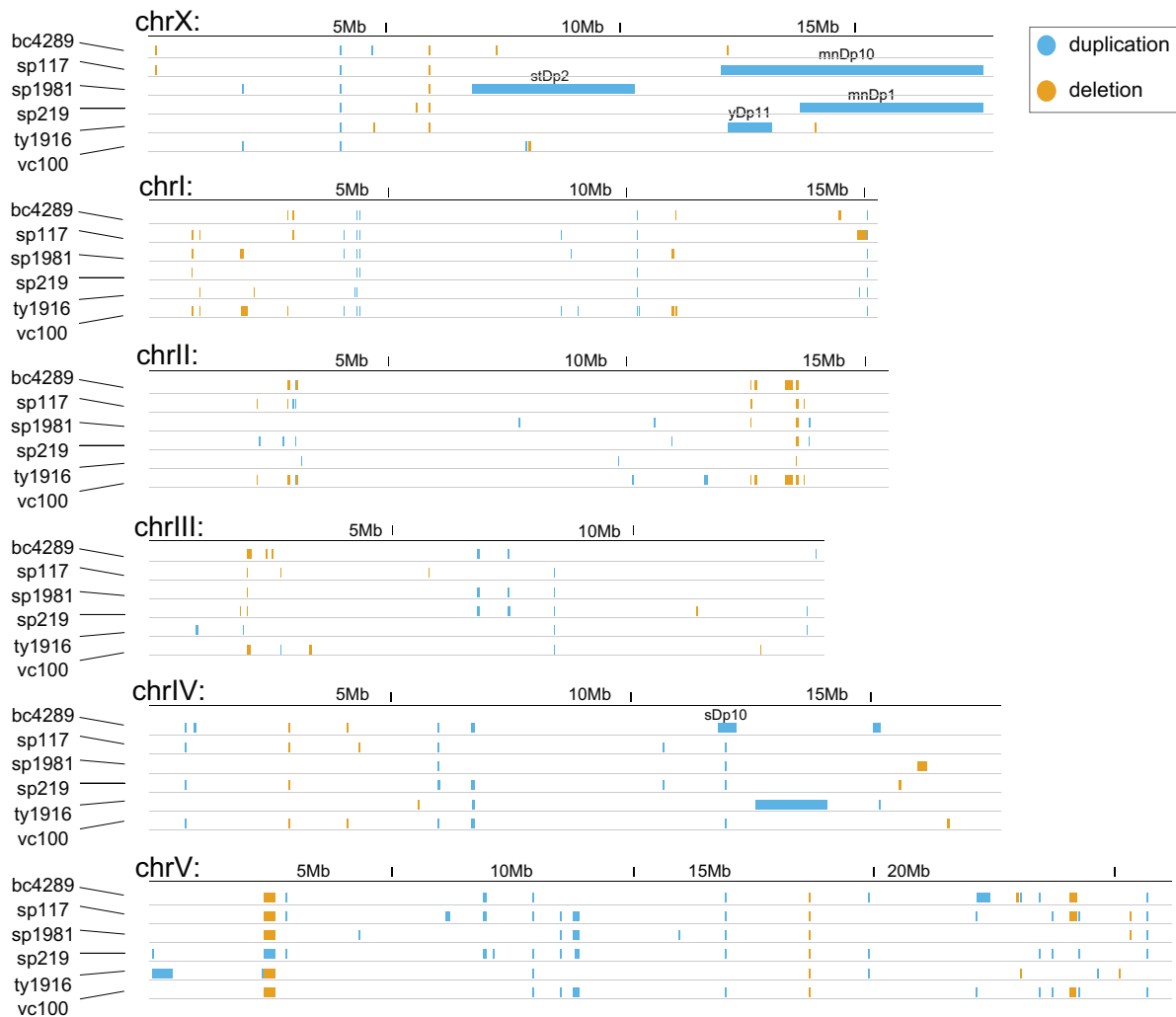


**Fig. 2.** CNVnator-identified duplications and deletions. CNVnator identified duplications and deletions from each strain are visualized across the whole genome. Output files for each strain are provided in Supplementary File 2. Duplications are shown as blue, and deletions are shown as orange bars. The previously characterized large chromosomal duplications are labeled in each strain.

similar with or without filtering (1.58 vs 1.51 for mnDp10, 2.34 vs 2.49 for yDp11, 1.51 vs 1.43 for duplication on chr IV in TY1916), thus lowly expressed genes did not significantly skew the analysis. We also plotted FPKM expression values for each gene between the large duplication strain SP117 and wild type (Supplementary Fig. 1b). Although the correlation is noisier at lower FPKM values, the shift in mRNA level is clear for genes located at the duplication.

To probe further into variability, we addressed if the tighter scatter of log<sub>2</sub> ratios on the X chromosome (Fig. 3) is due to lower expression noise, which was shown for the single X chromosome upregulated by the DCC in flies (Lee et al. 2018). To address noise, we calculated the coefficient of variation for each gene (filtering out those with FPKM < 1) using wild-type mRNA-seq data replicates in embryos, larvae, and young adults (Supplementary Fig. 1c). Overall, there was less variation in larvae, likely due to temporal dynamics of embryogenesis in embryos and germ cell development in young adults adding variability between collection of worms for mRNA-seq replicates. In all 3 developmental stages, the median coefficient of variation for X chromosomal genes was in between other chromosomes, suggesting that dosage compensation in worms does not reduce expression noise below that of autosomes.

### Increased mRNA expression and indirect effects of a multicopy integrated fosmid

While megabase-scale chromosome duplications showed an average increase in mRNA level, we wondered if smaller chromosomal segments with higher copy numbers also increase mRNA expression. To this end, we used a multicopy fosmid integration strain, where GFP-3xflag tag was inserted to the C terminus of *pha-4* gene within a fosmid containing 3 other genes (Sarov et al. 2012). The fosmid was then integrated into the genome randomly and a transgenic line that was vigorous and expressing the GFP-tagged *pha-4* was selected. This strain named OP37 was used to study the binding sites of *pha-4*, a transcription factor required for several developmental processes including the pharynx (Gaudet and Mango 2002; Zhong et al. 2010). The copy number for the fosmid was calculated to be 5.6 (Sarov et al. 2012).

The genes within and surrounding where the fosmid originated from are shown along with the DNA read coverage highlighting the increased gene dosage (Fig. 4a). The insertion site of the fosmid has not been mapped. Notably, the mRNA level of all 4 genes including *pha-4* was increased in the OP37 strain compared to N2 control (Fig. 4b). The increase for *pha-4* was by a factor of ~2.4 suggesting either feedback repression or an effect of



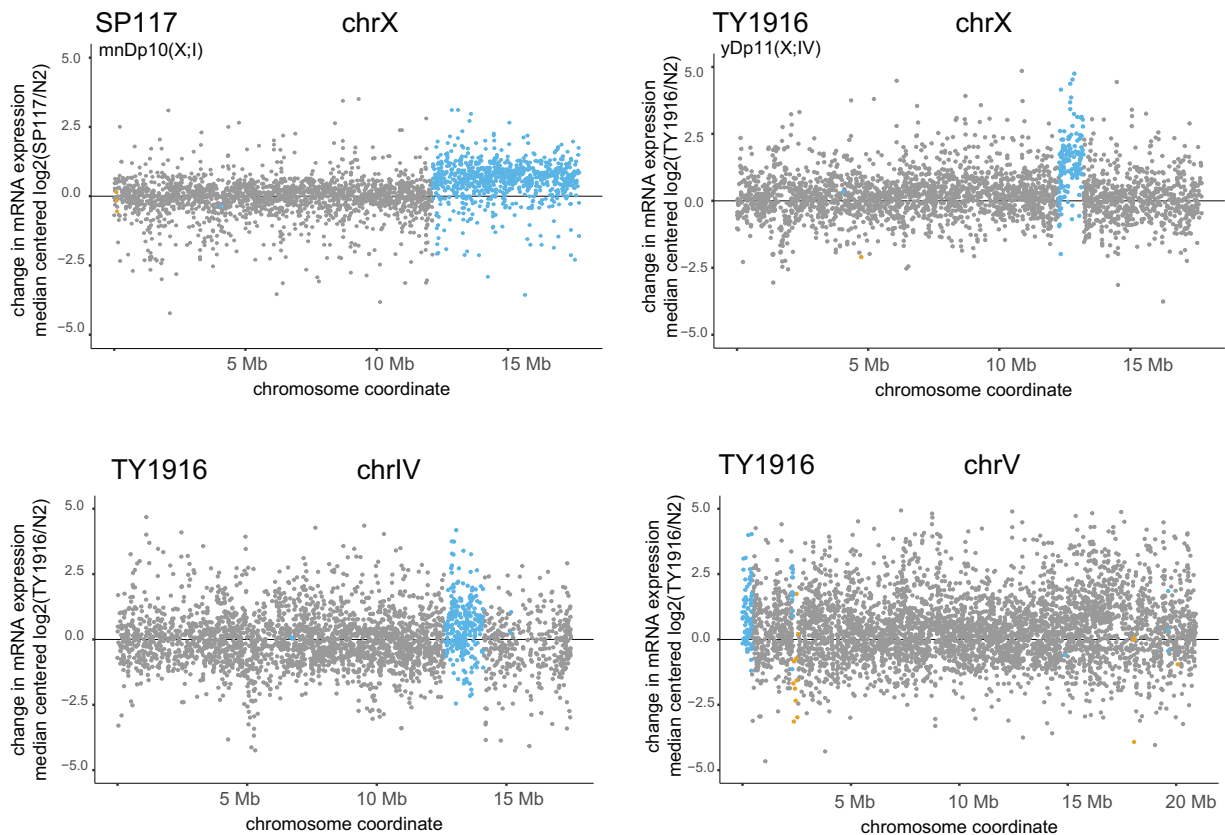


**Fig. 3.** mRNA-seq analysis of 4 duplicated regions in 2 strains. Changes in mRNA expression in the SP117 and TY1916 strains compared to N2 are shown. In each graph, the x-axis shows the entire chromosomes from which the duplications originated from. The y-axis is the genome-median centered log<sub>2</sub> ratio (mutant/N2) as determined by DESeq2. The DESeq2 outputs are provided in Supplementary File 4. The duplicated genes are highlighted in blue, deleted genes in orange, and unaffected genes in gray. Wilcoxon rank-sum test P-values are as follows: SP117 X duplicated versus X unaffected <math><2.2e-16</math>, TY1916 X duplicated versus X unaffected <math><2.2e-16</math>, TY1916 V-duplicated versus V-unaffected = 0.0016, TY1916 IV-duplicated versus IV-unaffected = 0.0029. Gene categories for all analyzed strains are provided in Supplementary File 3.

GFP tagging on mRNA expression or detection. The mRNA level of the other 3 genes on the fosmid increased by a factor of ~3.6- to 4.8, reflecting the increase in their copy number.

Highlighting the indirect effect on the transcriptome, 871 genes were identified to be up- or downregulated in the OP37 strain, despite the fosmid including only 4 genes. Analysis of genes that were differentially expressed revealed no enrichment for PHA-4 bound genes (25% of upregulated and 27% of downregulated genes were bound by PHA-4 compared to 27% of all genes; Fig. 4c). It is possible that ~2.4-fold increase in *pha-4* mRNA level does not cause an increase at the protein level or that the presence of multiple genes within the fosmid reduces *pha-4* specific changes on the transcriptome. The differentially expressed genes in the OP37 strain showed tissue-specific enrichment possibly reflecting the developmental functions of *pha-4* and the neighboring genes (Fig. 4d; Supplementary File 5).

### The mRNA increase from a X duplication differs across developmental stages

Next, we wondered how epigenetic regulation of the X chromosomes in different tissues would affect the consequence of an X chromosomal duplication. To address this question, we first considered the germline, where the X chromosomal genes are repressed compared to autosomal genes during early meiosis (Schaner and Kelly 2006). We reasoned that if a X chromosomal duplication is also subject to repression, the mRNA increase would be lower in adult worms. Indeed, genes located within the

5 Mb X chromosomal duplication in the SP117 strain showed less increase in mRNA expression in young adults compared to embryo and larvae (Fig. 5a). X chromosome repression in the germ cells is measurable in whole animals because germ cells outnumber the somatic cells in adults, leading to lower X chromosome expression compared to autosomes (Fig. 5b). Thus, our results suggest that repression of genes within the 5 Mb X chromosomal duplication in the germline negates the mRNA effect of the duplications specifically in this tissue.

The duplication strain BC4289 contains a ~1 Mb translocation from chromosome IV to X allowing us to test if autosomal genes attached to the X chromosome are repressed in germ cells. Unlike the 5 Mb X-to-I translocation in SP117, the 1 Mb IV-to-X translocation in BC4289 showed a similar increase in mRNA expression in young adults compared to larvae (Fig. 5c). Thus, germline repression may not affect autosomal genes even when they are physically attached to the X chromosome. In the future, multiple autosome to X duplications should be analyzed to test the generality of this conclusion. Nevertheless, the SP117 data suggest that epigenetic regulation of X chromosomal genes reduces the effect of a large X duplication on mRNA expression in the germline.

### Somatic dosage compensation reduces the level of mRNA increase in X chromosomal duplications

In *C. elegans*, hermaphrodite X chromosomes are repressed by a factor of 2 by somatic dosage compensation (Kramer et al. 2016). This repression is mediated by a condensin-based DCC that

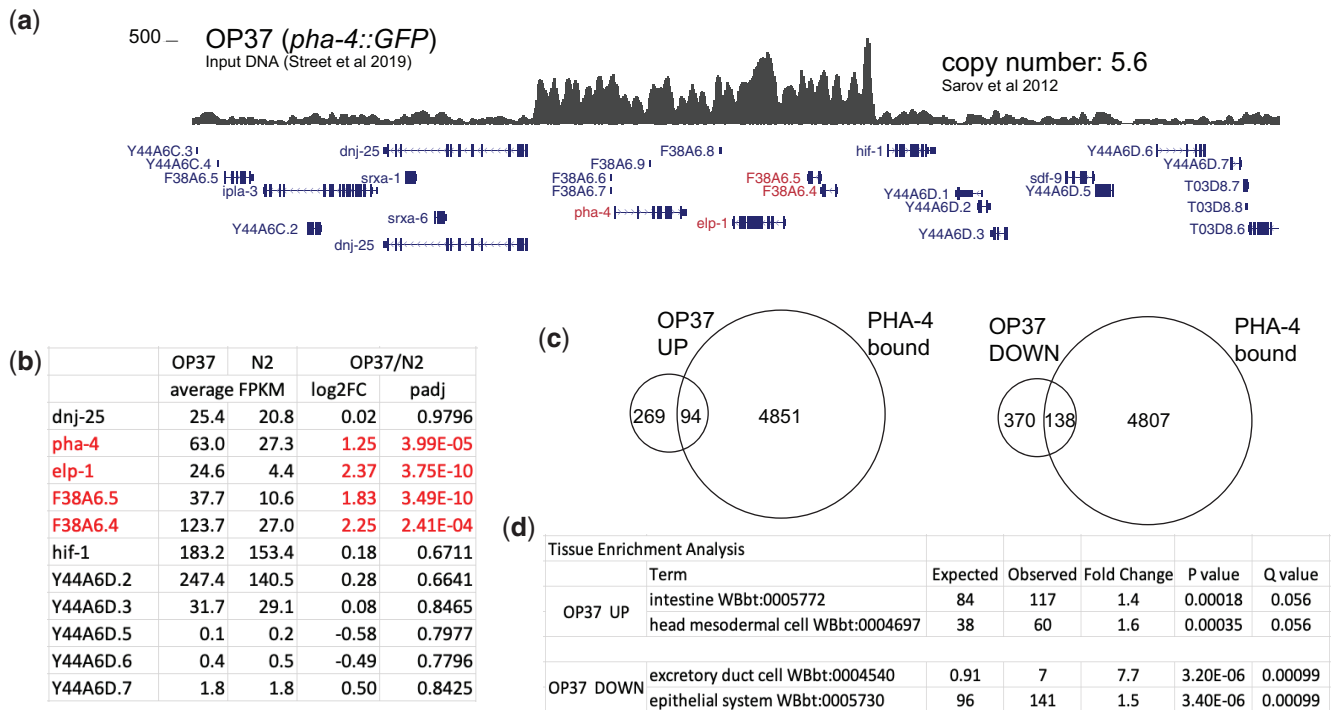


**Fig. 4.** mRNA-seq analysis in a multicopy integrated fosmid strain. a) DNA-seq read coverage plot of OP37 visualized on UCSC genome browser, centered at a ~70-kb window across the region where *pha-4* containing fosmid originated from. Genes included in the fosmid are highlighted in red. Only the longest isoforms are shown for simplicity. b) Table showing the average FPKM, log<sub>2</sub> fold change, and Padj values from DESeq2 analyses, listed for genes within and neighboring the *pha-4* containing fosmid. The genes within the fosmid are highlighted in red. The entire analysis is included in Supplementary File 4. c) Overlap of genes bound by PHA-4 (modENCODE ChIP-seq peaks at 1-kb promoters) and genes up- or downregulated in the OP37 strain compared to N2. d) Tissue enrichment analysis of differentially expressed genes in the OP37 strain. Top 2 categories are shown for up- and downregulated genes, and the rest are provided in Supplementary File 5.

specifically binds to and represses transcription initiation from both X chromosomes (Kruesi et al. 2013; Kramer et al. 2015). DCC is recruited specifically to the X chromosomes by several cis-regulatory elements on the X (McDonel et al. 2006; Ercan et al. 2007; Jans et al. 2009; Albritton and Ercan 2017). Recruitment leads to spreading of the complex to nearby chromatin, creating robust binding across the X chromosomes (Albritton et al. 2017; Street et al. 2019).

Previous studies used immunofluorescence to analyze the ability of several X chromosomal duplications to recruit the DCC (Csankovszki et al. 2004; Blauwkamp and Csankovszki 2009). These studies found that ~1Mb duplication in TY1916 (yDp11) does not recruit the DCC. Although one strong and one weak recruitment sites are present within yDp11, insertion of few recruitment elements is not sufficient to recruit high levels of DCC to an autosome (Albritton et al. 2017), explaining the lack of robust DCC binding to this shorter duplication. The same stretch of DNA within the larger ~5Mb duplication in SP117 (mnDP10), is bound by the DCC (Csankovszki et al. 2004), due to the additional ~4Mb region containing 5 strong and 15 weaker recruitment elements. Since genes in yDp11 are also in mnDP10, we were able to test if epigenetic repression by the DCC reduced the effect of increased dosage across the shared genes (Fig. 5d). Indeed, the average mRNA increase from the 1Mb region differed in the 2 strains (Fig. 5e). The median increase of mRNA expression from the 1Mb duplication was lower when bound by the DCC (SP117) compared to when unbound (TY1916).

In TY1916, there are 4 copies of genes located within the 1Mb yDp11; 2 X chromosomal copies under DCC-mediated repression and 2 duplicated copies on chromosome IV without DCC. In

SP117, all 4 copies of the genes within the commonly duplicated region between mnDp10 and yDp11 are under DCC-mediated repression. In both strains, the expected level of median mRNA increase (based on copy number and the assumed DCC repression by a factor of 2) was lower than that of observed; ~2.3-fold vs 3 in TY1916 and ~1.5-fold vs 2 in SP117 [after filtering genes (FPKM < 1) median increase was ~2.5 for TY1916 and 1.5 for SP117]. It would be interesting to know if other mechanisms of repression such as lamina-mediated organization of repressive chromatin contribute to repression of X chromosomal duplications (Snyder et al. 2016; Lee and Oliver 2018). Regardless, the lower level of mRNA increase from the same set of duplicated genes in the SP117 (DCC-bound) strain compared to TY1916 (DCC-unbound; Fig. 5f) indicates that DCC-mediated repression reduced the consequence of increased gene dosage on mRNA expression.

## Discussion

In *C. elegans*, several observations supported the idea that this organism is robust to changes in gene dosage in laboratory (Hodgkin 2005; Lipinski et al. 2011; Sarov et al. 2012; Konrad et al. 2018). Here, we showed that tolerance to increased gene dosage is not due to a genome-wide compensation mechanism acting at the mRNA level. However, it remains possible that effective mechanisms of compensation exist at the protein level (Dalley et al. 1993; Chang and Liao 2020). Post-transcriptional control of gene expression is common in *C. elegans* particularly in the germline (Nousch and Eckmann 2013), a tissue whose function is central to the viability of all isolated strains.

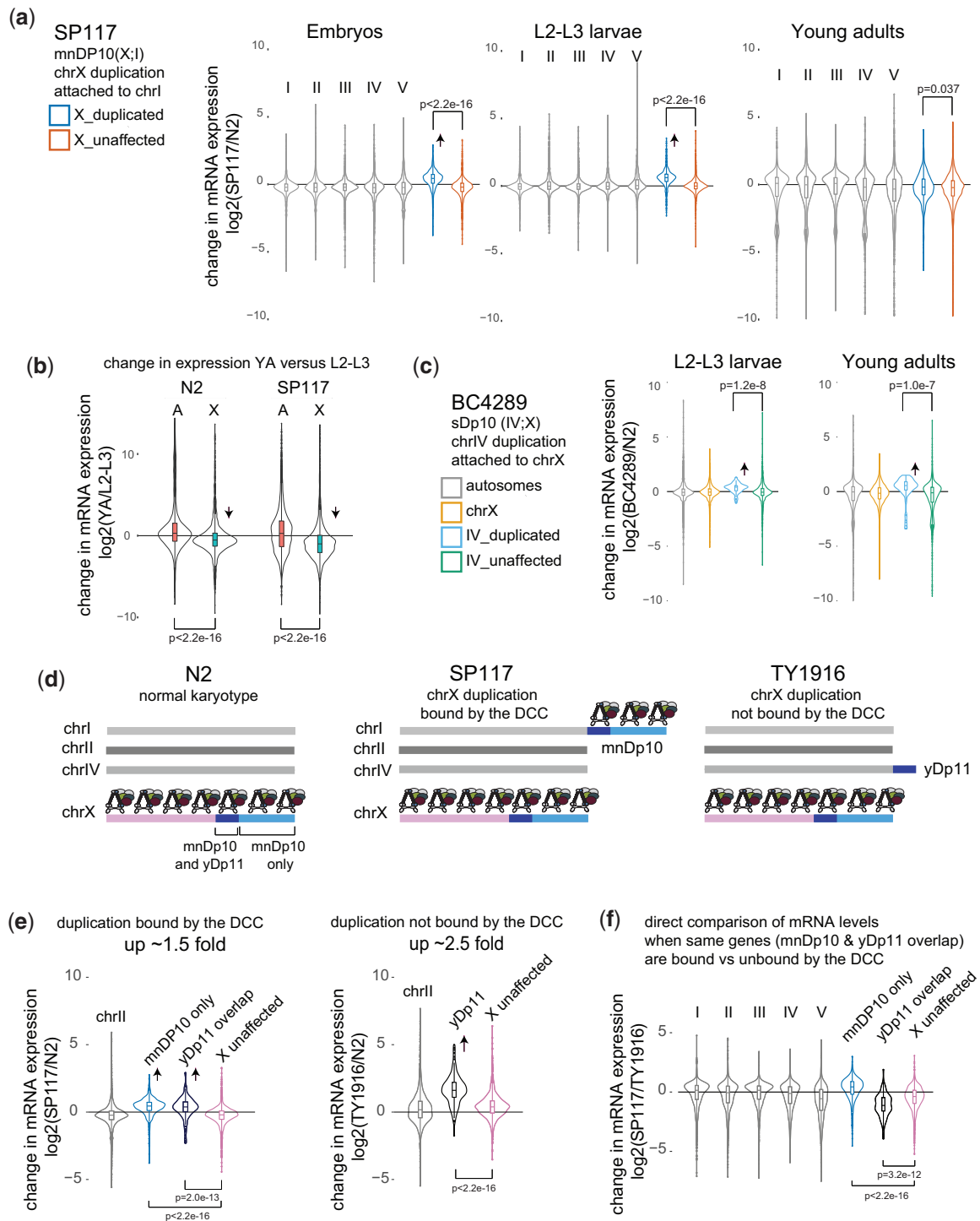


**Fig. 5.** mRNA expression in X duplications subject to repression in the soma and germline. a) SP117 contains a large ~5 Mb duplication of chr X that is attached to chr I. Violin plots of  $\log_2$  fold change from DESeq2 analysis of SP117 compared to N2 in embryos, L2-L3 larvae and young adult worms. Significance of difference between average  $\log_2$  fold change for genes within and outside the duplication from chr X is tested by t-test. Increased mRNA expression from the duplication in embryos and larvae is highlighted with an arrow. b) Violin plot of  $\log_2$  fold change from DESeq2 analysis of YA to L2-L3 in N2 and SP117. X chromosomes are repressed in the germ cells that are present in young adults but not in L2-L3 larvae. Difference in average change in expression between X and A is tested by t-test. c) BC4289 contains a ~1 Mb chr IV duplication attached to chr X. Violin plots of  $\log_2$  fold change from DESeq2 analysis of BC4289 compared to N2 in L2-L3 larvae and young adults is shown. Significance of difference between average  $\log_2$  fold change of genes within and outside the duplication from chr IV is tested using t-test. d) A schematic representing N2 control, SP117 and TY1916 genomes. The 1 Mb duplicated region (dark blue) in TY1916 (yDp11) does not bind to the somatic DCC. The 4 Mb uniquely duplicated region in SP117 (mnDp10) is indicated in light blue. Within mnDp10, genes within the duplicated region that overlap with yDp11 (dark blue) is bound by the DCC. e) Violin plots of  $\log_2$  fold change of SP117 and TY1916 compared to N2 in L2-L3 larvae. The 1.5- and 2.5-fold refer to the ratio of the median for the 1 Mb common duplicated region compared to the unaffected X chromosomal genes [lowly expressed genes (FPKM < 1)]. The arrows indicate the mRNA-seq increase in the duplicated regions, with P-values generated from t-test. f) Violin plot of  $\log_2$  fold change ratio for SP117 directly compared to TY1916. The increase in mRNA expression of the same set of genes is lower in SP117 when ~1 Mb X chromosome duplication is bound by the DCC compared to when unbound in TY1916.

Our analysis of chromosomal duplications in *C. elegans* indicates that similar to other organisms (Kojima and Cimini 2019), increased gene dosage leads to increased mRNA expression with a high degree of variability between genes (Fig. 3). The variation in response to gene dosage could be due to measurement errors based on technical and biological variation in mRNA expression. It could also be due to feedback through gene regulatory networks (Malone et al. 2012). Indirect effect of increased gene dosage on the transcriptome was particularly evident in the fosmid integration strain (Fig. 4). It is possible that compensatory changes in the expression of other genes render chromosomal duplications and CNVs viable in the laboratory.

Partial aneuploidies and CNVs in specific genes have been implicated in a wide range of diseases (Inaki and Liu 2012; Tang and Amon 2013; Durrbaum and Storchova 2016). To determine the cause and consequences of these CNVs on organism phenotypes, it is necessary to understand the variation both between genes and between tissues. Here, our results demonstrate that tissue-specific mechanisms of X chromosomal gene repression control the level of mRNA increase from certain duplications in the germline and the soma. Thus, increased gene dosage could result in varying levels of mRNA-seq increase, when the same set of genes is under different epigenetic regulation. Overall, our work adds *C. elegans* to the line of research analyzing partial aneuploidies, demonstrating a lack of genome-wide dosage compensation mechanism acting at the mRNA level, highlighting gene-to-gene variability and the contribution of epigenetic regulation to the mRNA response to gene dosage.

## Data availability

A list of new and published data used in this study is provided in Supplementary File 1 with GEO accession numbers. The new data are available at GEO Series number GSE198682. Supplementary Material is included at figshare: <https://doi.org/10.25387/g3.19762756>.

## Acknowledgments

The authors thank Marissa Knoll for contributing to the OP37 strain collection. Some strains were provided by the CGC, which is funded by NIH Office of Research Infrastructure Programs (P40 OD010440).

## Funding

Research reported in this publication was supported by National Institute of General Medical Sciences of the National Institutes of Health under award number R01GM107293 and R35GM130311.

## Conflicts of interest

None declared.

## Literature cited

- Abyzov A, Urban AE, Snyder M, Gerstein M. CNVnator: an approach to discover, genotype, and characterize typical and atypical CNVs from family and population genome sequencing. *Genome Res.* 2011;21(6):974–984.
- Afgan E, Baker D, Batut B, van den Beek M, Bouvier D, Cech M, Chilton J, Clements D, Coraor N, Grüning BA, et al. The Galaxy platform for accessible, reproducible and collaborative biomedical analyses: 2018 update. *Nucleic Acids Res.* 2018;46(W1):W537–W544.
- Aït Yahya-Graison E, Aubert J, Dauphinot L, Rivals I, Prieur M, Golfier G, Rossier J, Personnaz L, Creau N, Bléhaut H, et al. Classification of human chromosome 21 gene-expression variations in Down syndrome: impact on disease phenotypes. *Am J Hum Genet.* 2007;81(3):475–491.
- Albritton SE, Ercan S. *Caenorhabditis elegans* dosage compensation: insights into condensin-mediated gene regulation. *Trends Genet.* 2017;34(1):41–53.
- Albritton SE, Kranz A-L, Rao P, Kramer M, Dieterich C, Ercan S. Sex-biased gene expression and evolution of the x chromosome in nematodes. *Genetics.* 2014;197(3):865–883.
- Albritton SE, Kranz AL, Winterkorn LH, Street LA, Ercan S. Cooperation between a hierarchical set of recruitment sites targets the X chromosome for dosage compensation. *Elife.* 2017;6:e23645.
- Angeles-Albores D, Lee RYN, Chan J, Sternberg PW. Tissue enrichment analysis for *C. elegans* genomics. *BMC Bioinformatics.* 2016;17(1):366.
- Blauwkamp TA, Csankovszki G. Two classes of dosage compensation complex binding elements along *Caenorhabditis elegans* X chromosomes. *Mol Cell Biol.* 2009;29(8):2023–2031.
- Chang AY, Liao BY. Reduced translational efficiency of eukaryotic genes after duplication events. *Mol Biol Evol.* 2020;37(5):1452–1461.
- Csankovszki G, McDonel P, Meyer BJ. Recruitment and spreading of the *C. elegans* dosage compensation complex along X chromosomes. *Science.* 2004;303(5661):1182–1185.
- Dalley BK, Rogalski TM, Tullis GE, Riddle DL, Golomb M. Post-transcriptional regulation of RNA polymerase II levels in *Caenorhabditis elegans*. *Genetics.* 1993;133(2):237–245.
- Deng X, Hiatt JB, Nguyen DK, Ercan S, Sturgill D, Hillier LW, Schlesinger F, Davis CA, Reinke VJ, Gingeras TR, et al. Evidence for compensatory upregulation of expressed X-linked genes in mammals, *Caenorhabditis elegans* and *Drosophila melanogaster*. *Nat Genet.* 2011;43(12):1179–1185.
- Dossin F, Heard E. The molecular and nuclear dynamics of X-chromosome inactivation. *Cold Spring Harb Perspect Biol.* 2021;14(4):a040196.
- Durrbaum M, Storchova Z. Effects of aneuploidy on gene expression: implications for cancer. *FEBS J.* 2016;283:791–802.
- Edgley ML, Baillie DL, Riddle DL, Rose AM. Genetic balancers. In: *WormBook. The C. elegans Research Community, editor.* 2006. p. 1–32.
- Ercan S. Mechanisms of x chromosome dosage compensation. *J Genomics.* 2015;3:1–19.
- Ercan S, Giresi PG, Whittle CM, Zhang X, Green RD, Lieb JD. X chromosome repression by localization of the *C. elegans* dosage compensation machinery to sites of transcription initiation. *Nat Genet.* 2007;39(3):403–408.
- Farslow JC, Lipinski KJ, Packard LB, Edgley ML, Taylor J, Flibotte S, Moerman DG, Katju V, Bergthorsson U. Rapid increase in frequency of gene copy-number variants during experimental evolution in *Caenorhabditis elegans*. *BMC Genomics.* 2015;16:1044.
- Gasch AP, Hose J, Newton MA, Sardi M, Yong M, Wang Z. Further support for aneuploidy tolerance in wild yeast and effects of dosage compensation on gene copy-number evolution. *Elife.* 2016;5:e14409.
- Gaudet J, Mango SE. Regulation of organogenesis by the *Caenorhabditis elegans* FoxA protein PHA-4. *Science.* 2002;295(5556):821–825.



- Hodgkin J. Karyotype, ploidy, and gene dosage. In: WormBook. The *C. elegans* Research Community, editor. 2005. p. 1–9.
- Huettel B, Kreil DP, Matzke M, Matzke AJ. Effects of aneuploidy on genome structure, expression, and interphase organization in *Arabidopsis thaliana*. *PLoS Genet*. 2008;4(10):e1000226.
- Inaki K, Liu ET. Structural mutations in cancer: mechanistic and functional insights. *Trends Genet*. 2012;28(11):550–559.
- Jans J, Gladden JM, Ralston EJ, Pickle CS, Michel AH, Pferdehirt RR, Eisen MB, Meyer BJ. A condensin-like dosage compensation complex acts at a distance to control expression throughout the genome. *Genes Dev*. 2009;23(5):602–618.
- Kim D, Paggi JM, Park C, Bennett C, Salzberg SL. Graph-based genome alignment and genotyping with HISAT2 and HISAT-genotype. *Nat Biotechnol*. 2019;37(8):907–915.
- Kojima S, Cimini D. Aneuploidy and gene expression: is there dosage compensation? *Epigenomics*. 2019;11(16):1827–1837.
- Konrad A, Flibotte S, Taylor J, Waterston RH, Moerman DG, Bergthorsson U, Katju V. Mutational and transcriptional landscape of spontaneous gene duplications and deletions in *Caenorhabditis elegans*. *Proc Natl Acad Sci U S A*. 2018;115(28):7386–7391.
- Kramer M, Kranz A-L, Su A, Winterkorn LH, Albritton SE, Ercan S. Developmental dynamics of X-chromosome dosage compensation by the DCC and H4K20me1 in *C. elegans*. *PLoS Genet*. 2015;11(12):e1005698.
- Kramer M, Rao P, Ercan S. Untangling the contributions of sex-specific gene regulation and X-chromosome dosage to sex-biased gene expression in *Caenorhabditis elegans*. *Genetics*. 2016;204(1):355–369.
- Kruesi WS, Core LJ, Waters CT, Lis JT, Meyer BJ. Condensin controls recruitment of RNA polymerase II to achieve nematode X-chromosome dosage compensation. *Elife*. 2013;2:e00808.
- Kudron MM, Victorsen A, Gevirtzman L, Hillier LW, Fisher WW, Vafeados D, Kirkey M, Hammonds AS, Gersch J, Ammouri H, et al. The ModERN resource: genome-wide binding profiles for hundreds of *Drosophila* and *Caenorhabditis elegans* transcription factors. *Genetics*. 2018;208(3):937–949.
- Langmead B, Salzberg SL. Fast gapped-read alignment with Bowtie 2. *Nat Methods*. 2012;9(4):357–359.
- Lee H, Cho D-Y, Wojtowicz D, Harbison ST, Russell S, Oliver B, Przytycka TM. Dosage-dependent expression variation suppressed on the *Drosophila* male X chromosome. *G3 (Bethesda)*. 2018;8(2):587–598.
- Lee H, Oliver B. Non-canonical *Drosophila* X chromosome dosage compensation and repressive topologically associated domains. *Epigenetics Chromatin*. 2018;11(1):62.
- Li H. A statistical framework for SNP calling, mutation discovery, association mapping and population genetical parameter estimation from sequencing data. *Bioinformatics*. 2011;27(21):2987–2993.
- Lipinski KJ, Farslow JC, Fitzpatrick KA, Lynch M, Katju V, Bergthorsson U. High spontaneous rate of gene duplication in *Caenorhabditis elegans*. *Curr Biol*. 2011;21(4):306–310.
- Love MI, Huber W, Anders S. Moderated estimation of fold change and dispersion for RNA-seq data with DESeq2. *Genome Biol*. 2014;15(12):550.
- Malone JH, Cho D-Y, Mattiuzzo NR, Artieri CG, Jiang L, Dale RK, Smith HE, McDaniel J, Munro S, Salit M, et al. Mediation of *Drosophila* autosomal dosage effects and compensation by network interactions. *Genome Biol*. 2012;13(4):r28.
- McDonel P, Jans J, Peterson BK, Meyer BJ. Clustered DNA motifs mark X chromosomes for repression by a dosage compensation complex. *Nature*. 2006;444(7119):614–618.
- Meyer BJ. X-Chromosome dosage compensation. In: WormBook. The *C. elegans* Research Community, editor. 2005. p. 1–14.
- Nousch M, Eckmann CR. Translational control in the *Caenorhabditis elegans* germ line. *Adv Exp Med Biol*. 2013;757:205–247.
- Parkhomchuk D, Borodina T, Amstislavskiy V, Banaru M, Hallen L, Krobitch S, Lehrach H, Soldatov A. Transcriptome analysis by strand-specific sequencing of complementary DNA. *Nucleic Acids Res*. 2009;37(18):e123.
- Putri GH, Anders S, Pyl PT, Pimanda JE, Zanini F. Analysing high-throughput sequencing data in Python with HTSeq 2.0. *Bioinformatics*. 2022;38(10):2943–2945.
- Ramírez F, Ryan DP, Grüning B, Bhardwaj V, Kilpert F, Richter AS, Heyne S, Dündar F, Manke T. deepTools2: a next generation web server for deep-sequencing data analysis. *Nucleic Acids Res*. 2016;44(W1):W160–W165.
- Samata M, Akhtar A. Dosage compensation of the X chromosome: a complex epigenetic assignment involving chromatin regulators and long noncoding RNAs. *Annu Rev Biochem*. 2018;87:323–350.
- Sarov M, Murray JI, Schanze K, Pozniakovski A, Niu W, Angermann K, Hasse S, Rupprecht M, Vinis E, Tinney M, et al. A genome-scale resource for in vivo tag-based protein function exploration in *C. elegans*. *Cell*. 2012;150(4):855–866.
- Schaner CE, Kelly WG. Germline chromatin. In: WormBook. The *C. elegans* Research Community, editor. 2006. p. 1–14.
- Snyder MJ, Lau AC, Brouhard EA, Davis MB, Jiang J, Sifuentes MH, Csankovszki G. Anchoring of heterochromatin to the nuclear lamina reinforces dosage compensation-mediated gene repression. *PLoS Genet*. 2016;12(9):e1006341.
- Street LA, Morao AK, Winterkorn LH, Jiao C-Y, Albritton SE, Sadic M, Kramer M, Ercan S. Binding of an X-specific condensin correlates with a reduction in active histone modifications at gene regulatory elements. *Genetics*. 2019;212(3):729–742.
- Taggart JC, Li GW. Production of protein-complex components is stoichiometric and lacks general feedback regulation in eukaryotes. *Cell Syst*. 2018;7(6):580–589.e4.
- Tang YC, Amon A. Gene copy-number alterations: a cost-benefit analysis. *Cell*. 2013;152(3):394–405.
- Torres EM, Springer M, Amon A. No current evidence for widespread dosage compensation in *S. cerevisiae*. *Elife*. 2016;5:e10996.
- Trapnell C, Williams BA, Pertea G, Mortazavi A, Kwan G, van Baren MJ, Salzberg SL, Wold BJ, Pachter L. Transcript assembly and quantification by RNA-Seq reveals unannotated transcripts and isoform switching during cell differentiation. *Nat Biotechnol*. 2010;28(5):511–515.
- Vergara IA, Mah AK, Huang JC, Tarailo-Graovac M, Johnsen RC, Baillie DL, Chen N. Polymorphic segmental duplication in the nematode *Caenorhabditis elegans*. *BMC Genomics*. 2009;10:329.
- Zhang Y, Malone JH, Powell SK, Periwai V, Spana E, Macalpine DM, Oliver B. Expression in aneuploid *Drosophila* S2 cells. *PLoS Biol*. 2010;8(2):e1000320.
- Zhong M, Niu W, Lu ZJ, Sarov M, Murray JI, Janette J, Raha D, Sheaffer KL, Lam HYK, Preston E, et al. Genome-wide identification of binding sites defines distinct functions for *Caenorhabditis elegans* PHA-4/FOXA in development and environmental response. *PLoS Genet*. 2010;6(2):e1000848.